Journal of New Materials for Electrochemical Systems 21, 021-028 (2018)
© J. New Mat. Electrochem. Systems

Analysis of Redox Reactions on Pt-Sn based Nano-catalysts for Direct Methanol Fuel Cell Applications

A. Sandoval-González[1] and S.A. Gamboa[2,*]

[1]Centro de Investigación en Ingeniería y Ciencias Aplicadas, Universidad Autónoma del Estado de Morelos,
Av. Universidad 1001, Cuernavaca, Morelos 62209, Mexico.
[2]Instituto de Energías Renovables, Universidad Nacional Autónoma de México,
Privada Xochicalco s/n, Centro, 62580, Temixco, Morelos, México.

Received: October 06, 2017, Accepted: January 28, 2018, Available online: April 16, 2018

Abstract: *Low content Pt based catalysts (Pt-Mx, Mx: SnO_2, Sn) were prepared by microwave assisted-thermal synthesis. Pt-SnO_2/C catalyst showed good performance for methanol oxidation reaction. Besides, Pt_1Sn_1/C showed good performance for catalyzing the oxygen reduction reaction. The catalysts were characterized structurally by X-ray diffraction and transmission electron microscopy techniques. It was possible to observe the presence of nanoparticles obtained by the synthesis method used in this work. The chemical composition of every material was determined by energy dispersive spectroscopy analysis. The electrochemical characterization of the electrocatalytic materials was carried out in acid medium by cyclic voltammetry and rotating disk electrode techniques. Pt-SnO_2/C and Pt_1Sn_1/C were compared with commercial PtRu/C and Pt/C catalysts respectively. Pt-SnO_2/C showed better electrochemical characteristics than commercial PtRu/C for performing the methanol oxidation reaction (MOR). Pt_1Sn_1/C showed an exchange current density two orders of magnitude higher than commercial Pt/C for performing the oxygen reduction reaction (ORR). The materials were evaluated in an experimental direct methanol fuel cell (DMFC) operating during 10 hours. The electric power density loss showed by the DMFC made with commercial catalysts (PtRu/C and Pt/C) was 67% while the DMFC made with Pt-SnO_2/C and Pt_1Sn_1/C showed an electric power loss ca. 16%. It means that the catalysts synthesized in this work can be considered as good candidates for experimental direct methanol fuel cells.*

Keywords: Catalysts, methanol oxidation, oxygen reduction, Pt-SnO_2/C, Pt_1Sn_1/C, Direct methanol fuel cell

1. INTRODUCTION

Direct methanol fuel cells (DMFCs) have extensively been investigated due to their simple design and the facility for using alcohol as liquid fuel. Methanol is a cheap alcohol, easy to obtain as liquid fuel and it is safer to store and transport than hydrogen for PEM fuel cell applications. The use of a DMFC is limited principally due to the fast decay of the catalytic activity of the electrodes, it means that the performance of electrocatalyst is one of the impediments for the application of direct methanol fuel cells [1]. The problem occurs when methanol is oxidized on the electrocatalyst and at that moment some intermediate reactions take place at the surface of the active material. The most important reaction produces carbon monoxide (CO). This compound could be trapped on the surface of the electrocatalyst or in its chemical structure. When it occurs, the activity of the electrocatalyst diminishes rapidly as an irreversible reaction. The poisoning by CO affects the reaction onset and the oxidation of intermediate species requires more energy to complete the oxidation reaction. Platinum has been extensively studied for performing the redox reactions in direct methanol fuel cells, but Pt is easily poisoned by intermediate species during methanol oxidation. It is then necessary the addition of a second material to Pt for promoting the bifunctional process of adsorbed species. Platinum ruthenium supported on carbon (PtRu/C) is still considered as a better electrocatalyst than Pt/C for the methanol electrooxidation. PtRu is more tolerant to poisoning by the intermediate species during the methanol oxidation [2]. However, it is necessary to develop new materials with better tolerance characteristics to CO.

There are many studies indicating that SnO_2 added to Pt could be a better electrocatalyst for methanol oxidation reaction [3-11].

---

*To whom correspondence should be addressed: Email: sags@ier.unam.mx
Phone: +52 55 56229706; Fax.: +52 55 56229742

Higuchi et al [12] synthesized electrocatalysts with different Pt/Sn ratios by the modified Bönnemann method and they reported nanoparticles around 3.0 $\pm$ 0.5 nm and these electrocatalysts showed high specific activity and low overpotential for methanol oxidation reaction. Neto et al [13] prepared PtSn/C, PtRu/C and PtSnRu/C by alcohol reduction process and they discussed that PtSn/C based electrocatalyst showed better methanol oxidation characteristics than PtRu/C and PtSnRu/C. Guo and You [14] obtained platinum nanoparticles supported on sulphated SnO_2/multi-walled carbon nanotube composites (Pt-S-SnO_2/MWCNT) and this composite showed higher catalytic activity to oxidize methanol than commercial Pt/C and PtRu/C. Lim et al [15] synthesized PtSn/C nanoparticles by chemical reduction and hydrothermal treatment. The electrocatalyst was formed by nanoparticles of 2.3 nm. The methanol electrooxidation on PtSn/C occurred at overpotential lower than commercial Pt/C. It is believed that Sn has the capability to promote the oxidation of adsorbed CO at lower overpotential. Pang et al [16] prepared nanoparticles of Pt/Ru-doped SnO_2 and Pt/SnO_2 by chemical precipitation and thermal annealing at 823 K. Pt/Ru-doped SnO_2 showed better electrocatalytic activity than Pt/SnO_2 for a long-term cycling process. Zhang et al [17] synthesized SnO_2 nanoflowers and nanorods by hydrothermal method. These nanostructures were used as a support of Pt for methanol electrooxidation and flower-Pt/SnO_2 showed higher electrocatalytic activity and better long-term cycle stability than other electrocatalysts. Xu et al [18] synthesized IrO_2/SnO_2 by the Adams method for solid polymer electrolyte water electrolysis. The result showed that the catalytic properties of IrO_2/SnO_2 for the methanol oxidation were strongly dependent on the mass ratio of iridium to tin (2:1). Cui et al [19] synthesized Pt-SnO_2/GMC supported on graphitized mesoporous carbon (GMC) and they compared some results with Pt-SnO_2/C supported on commercial carbon black at the same electrocatalytic loading. Pt-SnO_2/GMC showed higher catalytic activity than Pt-SnO_2/C. Lin et al [20] synthesized Pt-SnO_2/CNTs at different Sn content. The methanol oxidation onset potential on Pt-SnO_2/CNTs was lower than Pt/C and the current density of the methanol oxidation on Pt-SnO_2/CNTs was two times higher than commercial Pt/C. These results indicate that SnO_2 needs to be investigated during the methanol oxidation reaction at different overpotentials [21].

The oxygen reduction reaction is a complex kinetic mechanism that has been extensively investigated during the last three decades. The oxygen can be reduced via two or four electrons forming hydrogen peroxide or water respectively [22]. In a direct methanol fuel cell, it is necessary that the oxygen reduction reaction occurs via four electrons for maximizing the transfer of electric power. Pt/C is still used for this application [23, 24] but it is very expensive and it is easy to be poisoned by intermediate species coming from the alcohol crossover through the membrane from the anode to the cathode of the fuel cell. There is a publication where PtSn/C is used for performing the oxygen reduction reaction [25].

In this work we propose the use of Pt-SnO_2/C like anodic electrocatalyst and Pt_1Sn_1/C like cathodic electrocatalyst for carrying out the redox reactions occurring in a direct methanol fuel cell. These electrocatalysts were synthesized by thermal heating using microwave irradiation at different conditions. The results indicate that both synthesized materials can be proposed for experimental fuel cells operating for a long time.

2. EXPERIMENTAL

2.1. Preparation of anodic and cathodic electrocatalysts and physical characterization

2.1.1. Synthesis of Pt-SnO_2/C as anodic electrocatalyst in a direct methanol fuel cell

Pt-SnO_2 based electrocatalyst was synthesized by thermal heating using microwave irradiation [26, 27]. It was formed a solution containing 0.039 mmol of chloroplatinic acid hexahydrate (H_2PtCl_6, sigma-Aldrich ^{TM} 99.9%), 0.35 mmol of stannous chloride dehydrate crystal ($SnCl_2$, J. T. Baker ^{TM} 99%) in 7.5 ml of ethylene glycol ($HOCH_2CH_2OH$, J.T. Baker 99.9%) and 7.5 ml of deionized water (18.2 MΩ-cm). The solution was then raised to pH 13 by adding 1 M sodium hydroxide (NaOH, Meyer 98.7%) drop wise by using a micropipette and it was vigorously stirred during 20 min at 25 °C. The pH value of the synthesis solution assured the formation of metallic oxidized species. The solution was placed in a reactor located inside the microwave synthesis device (Synthos 3000). The synthesis was carried out at 180 °C for 30 min. The product was filtered to obtain the electrocatalytic powder (Pt-SnO_2) and it was washed twice with deionized water at 80 °C and acetone (CH_3CH_3CO, Fermont 99.6%). At the end, the powder was dried at room temperature for 5 h following the experimental details discussed elsewhere [28].

2.1.2. Synthesis of Pt_1Sn_1/C as cathodic electrocatalyst in a direct methanol fuel cell

Pt_1Sn_1 based electrocatalyst was also synthesized by thermal heating using microwave irradiation. It was prepared a solution containing 0.096 mmol of chloroplatinic acid hexahydrate and 0.22 mmol of stannous chloride dehydrate crystal dissolved in 7.5 ml of ethylene glycol and 7.5 ml of deionized water. In this case, a pH 3 was adjusted for the solution by adding 1 M NaOH dropwise by using a micropipette. The synthesis of Pt_1Sn_1 was carried out in a Synthos 3000. It was followed the same experimental procedure as for the preparation of the anodic electrocatalyst.

Pt-SnO_2 and Pt_1Sn_1 nanoparticles were supported on Vulcan carbon XC-72 (Cabot) to obtain Pt-SnO_2/C and Pt_1Sn_1/C. Vulcan carbon shows the following characteristics: (1) high specific surface area of 250 $m^2\ g^{-1}$ and (2) because the commercial electrocatalysts used in this study as reference (Pt and PtRu) was supported on the same carbon, hence it is possible to compare results independent of the supporting material.

PtRu/C and Pt/C were acquired from E-TEK. The commercial electrocatalysts were used as reference materials for comparing the electrocatalytic performance of the materials synthesized in this work. It was possible to investigate the redox reactions occurring in an experimental DMFC. PtRu/C and Pt/C have the capability of catalyzing adequately the MOR and ORR respectively [29-34]. We consider that PtRu/C and Pt/C from E-TEK are good reference electrocatalysts for comparing the performance of new electrocatalytic materials for DMFC applications in acid medium.

The structural and morphological characterizations of Pt-SnO_2 and Pt_1Sn_1 nanoparticles was carried out by XRD, TEM and EDS. XRD analysis was performed by using a Rigaku DMAX-2200 diffractometer (Cu Kα1 radiation, 1.5406 Å). The XRD spectra were obtained from 5 to 100 degrees and the phases were identified with the software Jade 6.5. The Pt-SnO_2 and Pt_1Sn_1 nanoparticles were dispersed on Lacey C/Cu grids (300 mesh) and they were investigated by TEM analysis using a Jeol JEM2200FS Transmission Electron Microscope with STEM spherical aberration correction mode. Scanning transmission electron microscopy (STEM) technique is the most powerful microscope for characterizing the physicochemical nature of nanoscale systems. STEM instrument can provide complementary and unique information [35,36]. The chemical compositions of synthesized Pt-SnO_2 and Pt_1Sn_1 were investigated by EDS analysis using a Leo Scanning Electron Microscope model 1450VPS with an Oxford X-ray diffraction (Pentafet link) model 7366.

2.2. Electrochemical characterization

Catalytic inks were prepared for investigating the electrochemical characteristics of the synthesized nanoparticles. The inks were prepared by mixing 0.6 mg of metal powder (Pt-SnO_2, Pt_1Sn_1, PtRu or Pt), 1.4 mg of Vulcan XC-72 and 10 µL of 5% Nafion/isopropanol solution (ElectroChem). The solution in every case was sonicated for 5 min. It was possible to use this method to obtain supported electrocatalysts for electrochemical applications (Pt-SnO_2/C and Pt_1Sn_1/C). In each case, 1 µL of the catalytic ink was deposited as a thin layer on the surface of a glassy carbon disk held in a Teflon cylinder with a geometrical surface area of 0.071 cm^2. The thin layer was dried at room temperature for 15 minutes. The electrochemical studies were carried out at room temperature, in a conventional three compartment electrolytic cell with a water jacket for maintaining stable the temperature in the electrolyte. A mercury sulfate electrode (Hg/Hg_2SO_4/0.5 M H_2SO_4; K_2SO_4 sat.) was used as reference electrode (Ref 0.640 V vs. NHE). It was placed in a lugging capillary. A thick carbon rod was used as counter electrode. A solution of 0.5 M sulfuric acid (H_2SO_4 J.T. Baker 98%) and 1 M methanol (CH_3OH J.T. Baker 99.9%) was used as electrolyte for the analysis of methanol oxidation reaction. An oxygen-saturated solution of 0.5 M sulfuric acid was used as the electrolyte for the oxygen reduction studies. A potentiostat/galvanostat (Solartron Analytical, model SI 1287) and CorrWare^{TM} software were used for the electrochemical measurements and records of experiments.

2.3. Direct methanol fuel cell test

The catalytic inks used in the anode and cathode of the DMFC were prepared by mixing 2.5 mg of the electrocatalyst (Pt-SnO_2/C, Pt_1Sn_1/C, commercial PtRu/C or commercial Pt/C) with 30 µL of Nafion solution (Du Pont, 5 wt%, 1000EW, Electrochem) and 50 µl of isopropyl alcohol (J.T. Baker^{TM} 99.8 %). The mixture was placed in an ultrasonic bath (Branson 1510) for 1 hour for preparing the catalytic ink. The total amount of the prepared ink was used to cover 1 cm^2 area of the electrodes. The electrodes contained catalytic loading of 0.4 mg cm^{-2} of metal in anodes and cathodes. The catalytic inks were deposited directly on activated Nafion membrane by spraying at 80 °C [37,38]. At the anode side, it was used a Toray carbon diffuser and at the cathode side it was used a cloth carbon diffuser. The membrane-electrodes assembly was obtained by mechanical pressing at 100 kg cm^{-2} for 5 minutes at 100 °C. A direct methanol fuel cell of 1 cm^2 of apparent area was used for investigating the chemical to electrical energy conversion. 1 M methanol was supplied in the anode side of the fuel cell. 50 cc of oxygen was fed in the cathode side. It was possible to obtain the polarization plot of the cells by recording the I-V characteristic of the DMFCs. The experiments were performed at 25 ºC.

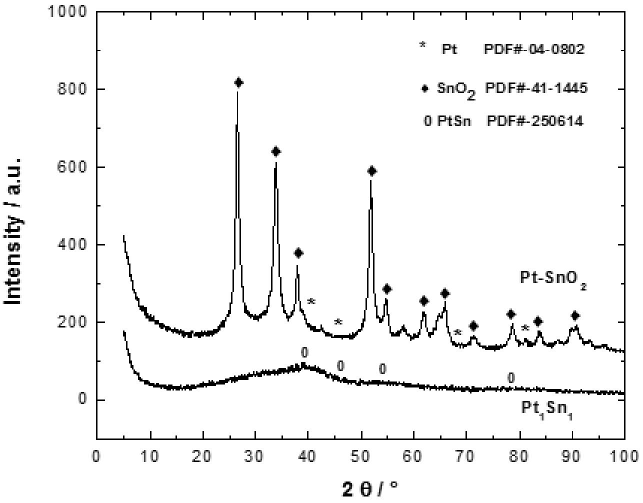

Figure 1. XRD patterns for Pt-SnO_2 and Pt_1Sn_1 catalysts.

3. RESULTS AND DISCUSSION

3.1. Structural analysis by XRD

Figure 1 shows the experimental XRD patterns of Pt-SnO_2. It is important to mention the co-existence of two crystalline phases (Pt and SnO_2). It was observed the presence of a nano-crystalline phase characterized for a broad diffraction area where defined peaks/planes were located at 26.54°/(110), 33.88°/(101), 37.88°/(200), 51.76°/(211), 54.739°/(220), 57.941°/(002), 61.959°/(310), 71.183°/(202), 78.796°/(321), 83.737°/(222) and 91.079°/(411). According to JCPDS file #41-1445, the previous planes correspond to SnO_2 tetragonal cassiterite phase. It was also observed the co-existence of Pt *fc*c phase at 39.96°, 46.04°, 67.8° y 81.7° (JCPDS file #04-0802). The calculated lattice parameters of SnO_2 were a=b=4.7456 Å and c=3.1833 Å values. Those values are different at the standard values obtained from JCPDS file #41-1445 where a=b=4.7382 Å and c=3.1871 Å. This difference could be attributed to the incorporation of Pt in the SnO_2 matrix. The estimated crystal size of SnO_2 was 5.6 nm (obtained by jade 6.5 software). It is expected that both phases, Pt and SnO_2 could complete the electro-oxidation reaction of methanol on the surface of the catalyst according to the bi-functional mechanism proposed by Feng et al [39]. In Figure 1 is also shown the XRD pattern for synthesized Pt_1Sn_1 and it is observed the nanometric nature of the electrocatalyst.

3.2. HRTEM analysis

In Figure 2 are shown the images obtained by TEM at low and high magnification for Pt-SnO_2 (Figure 2a and 2b respectively) and particle size distribution (Figure 2c). Figure 2a shows a typical low magnification TEM image of the sample and it is possible to observe well-defined spherical nanoparticles of Pt-SnO_2. The images show an adequate dispersion of nanoparticles and the calculated average particle size was 2.2 nm $\pm$ 0.2 nm. This result explains the broad area observed in XRD spectrum for Pt-SnO_2, it is indicating the presence of dispersed nanoparticles. The calculated inter-planar distance was 3.4 Å from the TEM image (Figure 2b) and we consider la formation of the system formed by Pt and SnO_2. It is possible according to the data available in the literature, the inter-planar

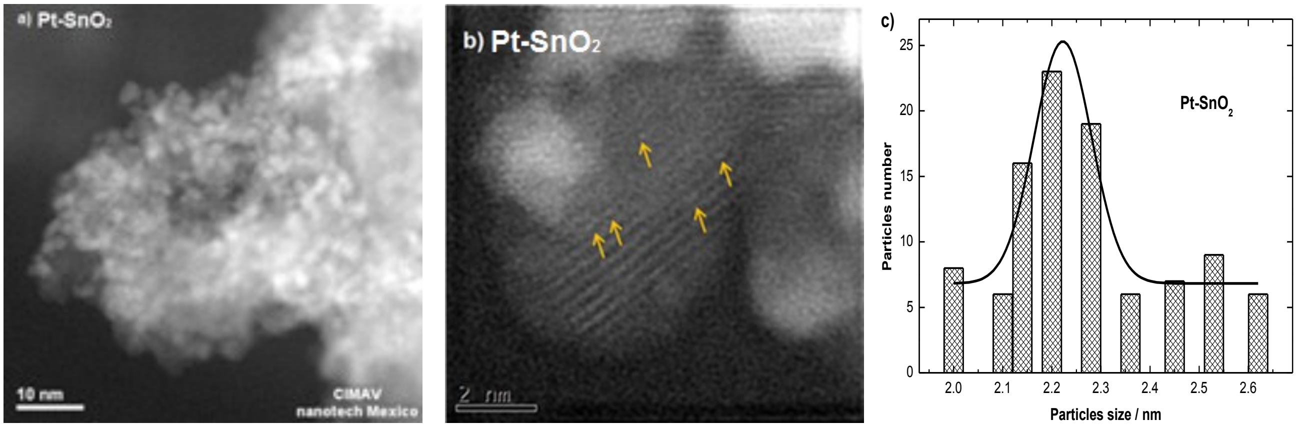

Figure 2. a) TEM image, b) HRTEM image and (c) histogram of particle size distribution for the synthesized Pt-SnO_2 electrocatalyst.

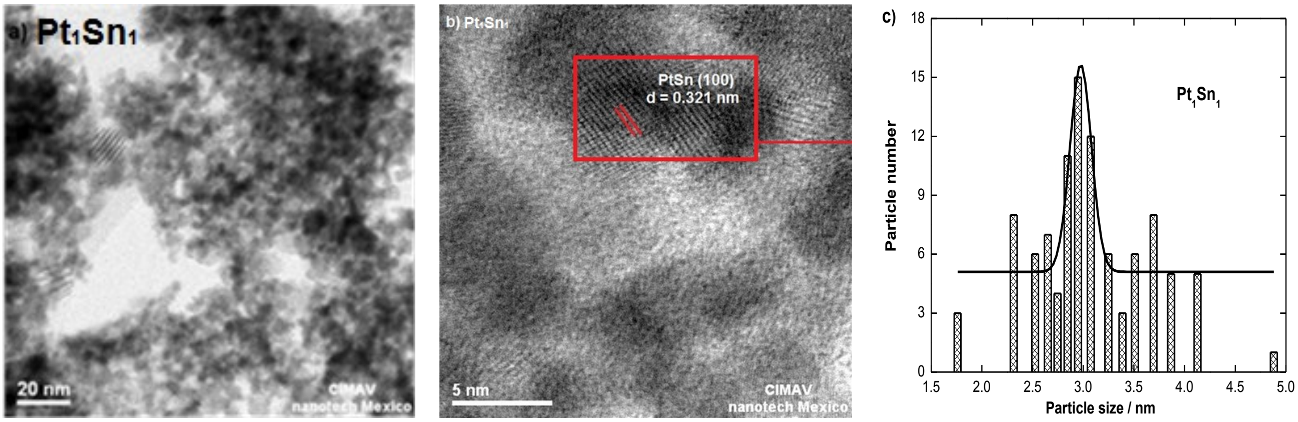

Figure 3. a) TEM image, b) HRTEM image and (c) histogram of particle size distribution for the synthesized Pt_1Sn_1 electrocatalyst.

distance for Pt is 3.921 Å (220) [40] and that for SnO_2 is 3.35 Å (110) [41]. This result indicates a possible incorporation of Pt in the matrix of SnO_2 because the atomic radius of Sn and Pt are 145 pm and 135 pm respectively [42]. In Figure 2b it is observed nanoclusters on the nanoparticle of SnO_2, we assume that those particles could be platinum. In Figure 3 are shown the TEM images and particle size distribution of Pt_1Sn_1 electrocatalyst. It was observed that the particles are spherical and uniformly distributed on the sample. HRTEM showed particles size around 3 $\pm$ 0.5 nm and it was corroborated with XRD. The inter-planar distance calculated by miller indices was 3.21 Å for Pt_1Sn_1. This result shows the presence of platinum and tin, in agreement with previous XRD results.

3.3. Analysis for determining the chemical composition

The chemical composition of commercial and synthesized electrocatalysts was investigated by EDS. The result showed that commercial PtRu/C contains more Pt than the sample of Pt-SnO_2 synthesized in this work. For PtRu/C, the atomic ratio (Pt:Ru) was 49.61:50.39. In this case, its stoichiometric proportion can be considered as almost 1:1 [43-44]. The composition analysis for Pt-SnO_2 showed a weight ratio (Pt:SnO_2) of 5.7:94.3. It is possible to consider that the atomic stoichiometric content of Pt in synthesized Pt-SnO_2 is almost 85% lower than E-TEK PtRu/C. Pt_1Sn_1 showed a wt.% chemical composition of 28:52 (Pt:Sn). There was no detection of oxygen in the sample due to the fast reduction process occurring during the synthesis, where oxygen was incapable of participating during the Pt-Sn reduction.

3.4. Electrochemical results

3.4.1. Methanol oxidation reaction

Figures 4 (a and b) shows the results of the methanol oxidation reaction on Pt-SnO_2/C and PtRu/C respectively. The experiments were performed in acid medium. The onset potential for performing the methanol oxidation reaction on Pt-SnO_2/C was 0.2 V/NHE and the onset potential of the reaction on commercial PtRu/C was 0.34 V/NHE. In this case, the lower threshold potential shown by Pt-SnO_2/C was a better electrocatalytic characteristic than commercial PtRu/C for carrying out the methanol oxidation reaction. Moreover, the oxidation potential on commercial PtRu/C showed a shift from 0.75 V/NHE in cycle 1 to 0.94 V/NHE at cycle 100. It means that the catalytic activity of PtRu/C decreases with time and it is needed more energy for oxidizing the methanol on PtRu/C due to adsorption of intermediate species on the surface of the catalyst. In the

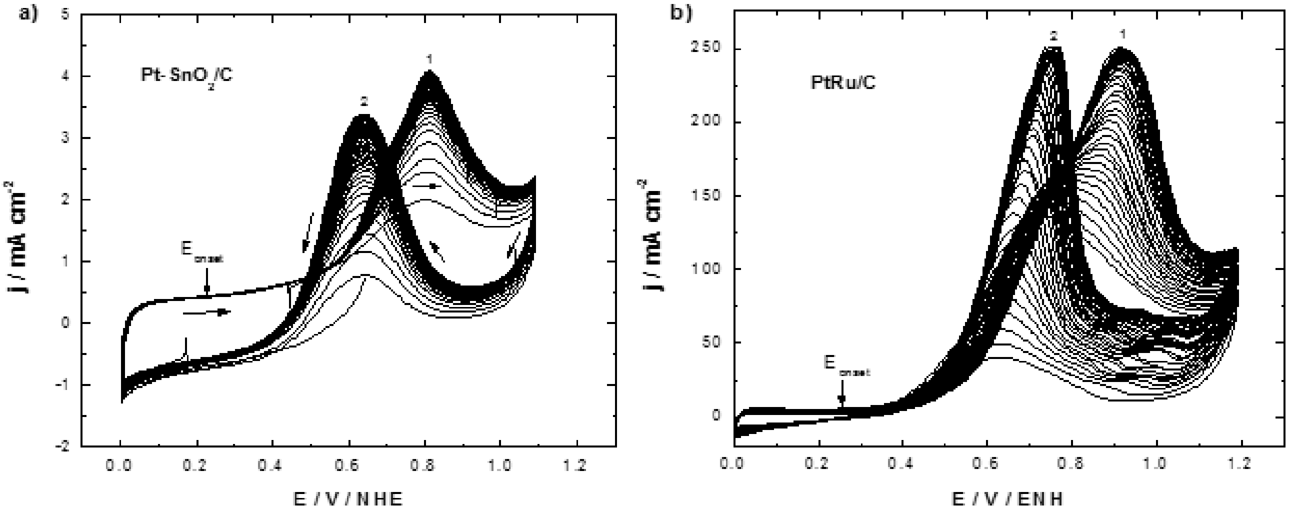

Figure 4. a) Methanol oxidation reaction on Pt-SnO_2/C and b) PtRu/C. 0.5 M H_2SO_4 + 1 M CH_3OH nitrogen saturated at 20 mV s^{-1} for 100 cycles. The experiments were carried out at room temperature.

case of Pt-SnO_2O/C the potential for the methanol oxidation remained the same during 100 cycles, indicating that the adsorption of intermediate species did not produce any significant affection on the catalytic activity of the material. Principal catalytic parameters were calculated for the methanol oxidation reaction on Pt-SnO_2O/C. The principal results were 400 $mVdec^{-1}$ for Tafel slope, 0.85 the charge transfer coefficient, 3.03 $X10^{-3}$ $mAcm^{-2}$ the exchange current density and 0.104 cm^{-2} the electrochemical active area. The parameters obtained from the methanol oxidation on Pt-SnO_2/C indicated that the kinetic mechanism was controlled by the formation of metallic oxide and one electron transition during the bi-functional process for oxidizing CH_3OH and it was probably activated by the co-existence of a SnO_2 phase. The electrochemical mechanism for the oxidation reaction of methanol on Pt-SnO_2O/C follows the reactions (1) and (2) [48]:

$$SnO_2 + H_2O \rightarrow SnO_2 - OH_{ads} + H^+ + e^- \tag{1}$$

$$Pt - CO_{ads} + SnO_2 - OH_{ads} \rightarrow Pt + SnO_2 + CO_2H^+ + e^- \tag{2}$$

It was not possible to investigate the kinetic characteristics of commercial PtRu/C because it showed instability during the methanol oxidation reaction.

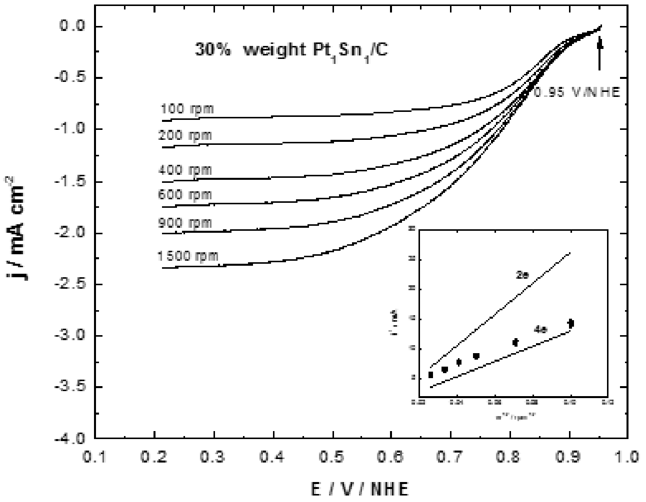

Figure 5. Oxygen reduction reaction on Pt_1Sn_1/C. Oxygen saturated 0.5 M H_2SO_4, 5 mV s^{-1}. The experiments were carried out at room temperature.

3.4.2. Oxygen reduction reaction

In figure 5 it is shown the oxygen reduction reaction on Pt_1Sn_1/C at room temperature. The experiments were carried out from 100 to 1500 rpm of scan rate to obtain kinetic information from the ORR. The reduction reaction threshold occurred at 0.95 V/NHE. The j-E plots at different scan rates were stable and dependent of the convection process. The reaction mechanism in this case involved the transfer of 4 electrons for forming water and it was corroborated by analyzing the tendency of the limiting current vs scan rate [45-47]. In Table 1 are shown the kinetic parameters, Tafel slope, charge transfer coefficient, exchange current density and specific electrochemical area of commercial Pt/C and Pt_1Ru_1/C that was synthesized in this work. The results showed that Pt_1Sn_1/C was a better catalyst than Pt/C for reducing oxygen at the established condi-

Table 1. Kinetics parameters obtained from the oxygen reduction reaction on Pt_1Sn_1/C.

Electrocatalyst	b mV dec^{-1}	α	i_0 mA cm^{-2}	A_{ea} cm^2
Commercial Pt/C	-115	-0.51	$7.22x10^{-6}$	0.099
Pt_1Sn_1/C	-117	-0.51	$1.83x10^{-4}$	0.149

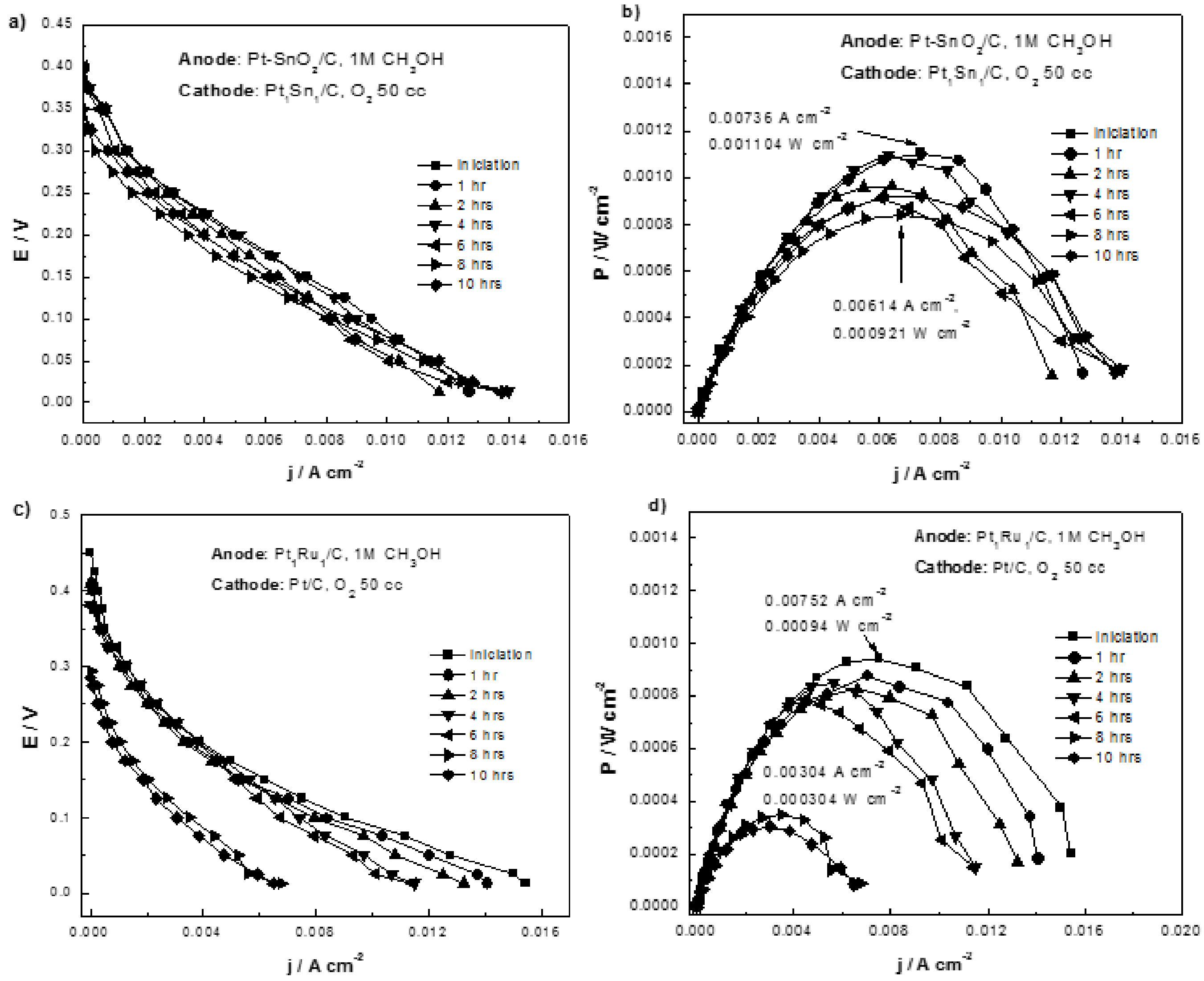

Figure 6. Electric characterization of experimental DMFCs. Synthesized catalysts: a) I-V characteristic, b) Electric power density. Commercial catalysts: c) I-V characteristic, d) Electric power density

tions. The results also indicated that the kinetic current on Pt_1Sn_1/C was two orders of magnitude higher than Pt/C, with this result we consider that a higher value in exchange current density assures the transfer of 4 electrons during the ORR and it contributed to better I-V characteristics when the experimental fuel cell was operating at room temperature.

3.4.5. Direct methanol fuel cell performance

Two DMFCs were prepared in the lab by using the catalysts discussed in this work. The fuel cells were operating during 10 hr at room temperature. The liquid and gas fluxes containing the fuel and oxidant were at a constant ratio of 100 cc/methanol and 80 cc/O_2. One DMFC was operating with the catalysts synthesized in this work and the results are shown in figure 6(a), Figure 6(b). The other one was made with commercial catalysts and the results are shown in Figures 6(c) and Figure 6(d). In Figure 6(a) is shown the I-V polarization of the direct methanol fuel cell where Pt-SnO_2/C was used like anodic catalyst and Pt_1Sn_1/C as cathodic catalyst. The maximum voltage recorded at the initial operation conditions was 0.40 V and it was obtained a maximum current density of ca. 0.014 Acm^{-2}. The I-V data were recorded every two hr during the experiment time. The electric power of this DMFC diminished ca. 16% during 10 hr of continuous operation as can be observed in Figure 6(b). The performance of this DMFC remains almost constant. It means that the catalysts used in this fuel cell are adequate for carrying out the redox reaction for producing steadily electric power at room temperature. In Figure 6(c) is shown the I-V characteristic of the DMFC made with commercial catalysts. The initial voltage was recorded as 0.45 V and its corresponding maximum current density was 0.015 Acm^{-2}. The fuel cell was also operating during 10 hr and it was observed a drastic decay in I-V characteristic after 6 hr of operation and the calculated power density decay was more than 67% in this DMFC. It means that the commercial catalysts PtRu/C and Pt/C for anodic and cathodic reactions respectively are strongly affected by intermediate species during the methanol oxidation during the first 6 hr of operation. The evaluation of the catalysts in an experimental DMFC showed that Pt-SnO_2/C and Pt_1Sn_1/C can be considered as promising catalysts to be used in long-term operation DMFCs.

4. CONCLUSION

Pt-SnO_2/C catalyst was properly prepared by thermal heating using microwave irradiation. This material was formed by two structural phases with low Pt content. The material was nanostructured with a mean particle size of 5.6 nm. Pt-SnO_2/C showed adequate properties for performing the methanol oxidation reactions. The calculated kinetic parameters for MOR showed better catalytic characteristics than PtRu/C. On the other hand, Pt_1Sn_1/C was also prepared by thermal heating using microwave irradiation and this material showed better kinetic parameters for performing the ORR than commercial Pt/C. The kinetic results were proved in the performance of experimental DMFCs. Pt-SnO_2/C and Pt_1Sn_1/C are promising catalysts for DMFC applications.

5. ACKNOWLEDGMENTS

Authors want to thank Dr. Francisco Paraguay-Delgado from CIMAV-Mexico for his support for the samples characterization by HRTEM. Authors are also grateful to thank CONACYT Grants 128545, DGAPA PAPIIT IN111011 and IN112217 to support this project.

REFERENCES

[1] Badwal, S. P. S., Giddey, S., Kulkarni, A., Goel, J., Basu, S. Appl. Energy, 145, 80 (2015).

[2] Taufany, F. Pan C, Lai F, Chou H, Subramanyam Sarma L., Rick J., Lin J, Lee J., Tang M., Hwang B., Chem. -A Eur. J. 19, 905 (2013).

[3] Y. Fan, J. Liu, H. Lu, P. Huang, D. Xu, Electrochim. Acta, 76, 475 (2012).

[4] Chen G., Du L., Du C., Kong F., Sun Y., Qian Z., Yin G., Gao Y., Electrochemistry, 85, 2016 (2017).

[5] Zheng Y., Zhan H., Fang Y., Zeng J., Liu H., Yang J., Liao S., J. Mater. Sci., 52, 3457 (2017).

[6] Ju H. K., Giddey S., Badwal S. P. S., Electrochim. Acta, 229, 39 (2017).

[7] Sethu S. P., Gangadharan S., Chan S. H., Stimming U., J. Power Sources, 254, 161 (2014).

[8] S.G. Ramos, A. Calafiore, A.R. Bonesi, W.E. Triaca, A.M. Castro Luna, M.S. Moreno, G. Zampieri, S. Bengio, Int. J. Hydrogen Energy, 37, 14849 (2012).

[9] Yousaf A. Bin, Imran M., Kasak P., Sifani Zavahir F., Javaid Zaidi S., Fernandez C., Catal. Sci. Technol., 7, 3283 (2017).

[10]Lu S., S Eid, K. Ge, D. Guo, J. Wang, L. Wang, H. Gu, Nanoscale, 1033 (2016).

[11]G.R. Salazar-Banda, H.B. Suffredini, L.A. Avaca, S.A.S. Machado, Mater. Chem. Phys., 117, 434 (2009).

[12]E. Higuchi, K. Miyata, T. Takase, H. Inoue, J. Power Sources, 196, 1730 (2011).

[13]A. Oliveira Neto, R.R. Dias, M.M. Tusi, M. Linardi, E.V. Spinacé, J. Power Sources, 166, 87 (2007).

[14]D.J. Guo, J.M. You, J. Power Sources, 198, 127 (2012).

[15]D.H. Lim, D.H. Choi, W.D. Lee, H.I. Lee, App. Catal., B., 89, 484 (2009).

[16]H.L. Pang, X.H. Zhang, X.X. Zhong, B. Liu, X.G. Wei, Y.F. Kuang, J.H. Chen, J. Colloid Interface Sci., 319, 193 (2008).

[17]H. Zhang, C. Hu, X. He, L. Hong, G. Du, Y. Zhang, J. Power Sources, 196, 4499 (2011).

[18]J. Xu, G. Liu, J. Li, X. Wang, Electrochim. Acta, 59, 105 (2012).

[19]X. Cui, F. Cui, Q. He, L. Guo, M. Ruan, J. Shi, Fuel., 89, 372 (2010).

[20]Y. Lin, S. Zhang, S. Yan, G. Liu, Electrochim. Acta, 66, 1 (2012).

[21]A. Sandoval-González, E. Borja-Arco, Jaime Escalante, O. Jiménez-Sandoval, S.A. Gamboa, Int. J. Hydrogen Energy, 37, 1752 (2012).

[22]G. Girishkumar, K. Vinodgopal, P.V. Kamat, J. Phys. Chem. B., 108, 19960 (2004).

[23]M. Lefévre, J.-P. Dodelet, Electrochim. Acta, 48, 2749 (2003).

[24]D.H. Jung, S.J. Bae, S.J. Kim, K.S. Nahm, P. Kim, Int. J. Hydrogen Energy, 36, 9115 (2011).

[25]C. Jeyabharathi, P. Venkateshkumar, J. Mathiyarasu, K.L.N. Phani, Electrochim. Acta, 54, 448 (2008).

[26]M. Sakthivel, A. Schlange, U. Kunz, T. Turek, J. Power Sources, 195, 7083 (2010).

[27]C.O. Kappe, D. Dallinger, S.S. Murphree, Practical Microwave Synthesis for Organic Chemists: Strategies, Instruments and Protocols, Wiley-VCH Capitulo 2, 2009.

[28]E. Antolini, T. Lopes, E.R. Gonzalez, J. Alloys Compd., 461, 253 (2008).

[29]W. Vogel, J. Phys. Chem. C., 112, 13475 (2008).

[30]J.W. Guo, T.S. Zhao, J. Prabhuram, R. Chen, C.W. Wong, Electrochim. Acta, 51, 754 (2005).

[31]F. Colmati, W.H. Lizcano-Valbuena, G.A. Camara, E.A. Ticianelli, E.R. Gonzalez, J. Braz, Chem. Soc., 13, 474 (2002).

[32]P. Selvam, B. Kuppan, Catal. Today, 198 85 (2012).

[33]H.X. Huang, S.X. Chen, C. Yuan, J. Power Sources, 175, 166 (2008).

[34]L. Calvillo, M. Gamgeri, S. Perathoner, G. Centi, R. Moliner, M.J. Lázaro, Int. J. Hydrogen Energy, 36, 9805 (2011).

[35]A. Uzun, V. Ortalan, Y. Hao, N.D. Browning, B.C. Gates, ACS Nano., 3, 3691 (2009).

[36]J. Liu, J. Electron Mycroscopy, 54, 251 (2005).

[37]J. Mann, N. Yao, A.B. Bocarsly, Langmuir, 22, 10432 (2006).

[38]B. Thoben, A. Siebke, J. New Mat. Electrochem. Systems, 7, 13 (2004).

[39]Y. Feng, L. Jingjing, W. Tongtao, L. Yun, W. Haojie, L. Jianling, J. Phys. Chem. C., 112, 12894 (2008).

[40]Z. Liu, B. Guo, L. Hong, T. Han Lim, Electrochem. Commun.,

8, 83 (2006).

[41]D. Chen, L. Gao, Chem. Phys. Lett., 398, 201 (2004).

[42]J.C. Slater, J. Chem. Phys., 41, 3199 (1964).

[43]F. Colmati, W.H. Lizcano-Valbuena, G.A. Camara, E.A. Ticianelli, E.R. Gonzalez, J. Braz. Chem. Soc., 13, 474 (2002).

[44]W.C. Chang, M.T. Nguyen, J. Power Sources, 196, 5811 (2011).

[45]S. Treimer, A. Tanga, D.C. Johnson, Electroanalysis, 14(3), 165 (2002).

[46]A.J. Bard, R. Parsons, J. Jordan. Standard potentials in aqueous solution (prepared under the auspices of the International Union of Pure and Applied Chemistry), Marcel Dekker, New York, 1985.

[47]A.J. Bard, L. Faulkner. Electrochemical Methods: Fundamentals and Applications, Wiley, New York, 2001.

[48]F. Ye, J. Li, T. Wang, Y. Liu, H. Wei, J. Li, X. Wang, J. Phys. Chem. C, 112, 12894 (2008).